

# CMB polarization induced by stochastic magnetic fields

Massimo Giovannini<sup>a,c</sup> and Kerstin E. Kunze<sup>b,c</sup>

<sup>a</sup>*INFN, Section of Milan-Bicocca, 20126 Milan, Italy*

<sup>b</sup>*Departamento de Física Fundamental,  
Universidad de Salamanca, Plaza de la Merced s/n, E-37008 Salamanca, Spain*

<sup>c</sup>*Department of Physics, Theory Division, CERN, 1211 Geneva 23, Switzerland*

## Abstract

The complete calculation of the CMB polarization observables (i.e. E- and B-modes) is reported within the conventional  $\Lambda$ CDM paradigm supplemented by a stochastic magnetic field. Intriguing perspectives for present and forthcoming CMB polarization experiments are outlined.

Large-scale magnetism recently became an intriguing triple point where cosmology, astronomy and high-energy astrophysics meet for complementary purposes [1]. Still we have no clues on its origin. The gravitational instability together with the subsequent galactic rotation could amplify a magnetic field spanning a collapsing region of the order of the Mpc in comoving units. The magnetic field regularized over such a scale  $L$ , i.e.  $B_L$ , is not empirically observable at the epoch of the gravitational collapse of the protogalaxy. But the Universe is a good conductor: the magnetic flux and helicity are approximately conserved implying that large-scale magnetic fields could have been already present at the time when photons last-scattered electrons and ions, i.e., according to the WMAP 5-year data [2], at a redshift  $z_{\text{dec}} \simeq 1090$ .

Intriguing effects related to tangled magnetic fields have been discussed with semi-analytical methods (see, in particular, [3]). More recently the impact of large-scale magnetic fields on scalar modes of the geometry have been addressed [4] and a dedicated numerical approach has been devised [5]. The complete calculation of the polarization angular power spectra (i.e., specifically, the EE, TE and BB angular power spectra) is here reported, for the first time, when the conventional  $\Lambda$ CDM paradigm is complemented by a stochastic magnetic field (i.e., according to the terminology of [5], m $\Lambda$ CDM scenario).

In short the main theoretical impasse is the following. The large-scale description of temperature anisotropies demands a coarse grained (one-fluid) approach for the electron-ion system: this is the so called baryon fluid which is treated (with no exceptions) as a single fluid in popular Boltzmann solvers such as COSMICS [6] and CMBFAST [7]. On the other hand the dispersive propagation of electromagnetic disturbances demands to treat separately electrons and ions, at least at high frequencies. It is appropriate to start from the Vlasov-Landau equation written in the form:

$$\frac{\partial f_{\pm}}{\partial \tau} + v^i \frac{\partial f_{\pm}}{\partial x^i} \pm e(E^i + v_j B_k \epsilon^{jk i}) \frac{\partial f_{\pm}}{\partial q^i} + \frac{1}{2} h'_{ij} q^i \frac{\partial f_{\pm}}{\partial q^j} = \mathcal{C}_{\text{coll}}. \quad (1)$$

where  $\vec{v} = \vec{q}/\sqrt{m^2 a^2 + q^2}$  is the comoving three velocity,  $\vec{q}$  is the comoving three-momentum and  $\tau$  is the conformal time arising, in the line element, as  $ds^2 = a^2(\tau)\{d\tau^2 - [\delta_{ij} - h_{ij}(\vec{x}, \tau)]dx^i dx^j\}$ . The prime denotes a derivation with respect to  $\tau$ . The rescaled electromagnetic fields are denoted as  $\vec{E} = a^2 \vec{\mathcal{E}}$  and as  $\vec{B} = a^2 \vec{\mathcal{B}}$ . By choosing the plus (minus) sign in Eq. (1), the evolution equation for the one-body distribution function  $f_{\pm}(\vec{x}, \vec{q}, \tau)$  of the ions (electrons) can be obtained<sup>1</sup>. In the electron-ion system  $\mathcal{C}_{\text{coll}}$  is provided by Coulomb scattering.

In the limit  $e \rightarrow 0$ , Eq. (1) describes the evolution of neutral species. If  $\mathcal{C}_{\text{coll}} = 0$ , Eq. (1) leads, below the MeV, to the well known evolution equation for the reduced phase space

---

<sup>1</sup>The velocity-configuration space naturally arises since ions and electrons are all non-relativistic. Consequently, the comoving three-momentum is given by  $\vec{q} = m\vec{v}$  for each of the two charged species. The quasi-equilibrium distribution for electrons and protons is Maxwellian and the strength of Coulomb scattering guarantees  $T_e \simeq T_i \simeq T$ . For relativistic (neutral) species  $q^i = n^i q$ . The equilibrium distribution for neutrinos and photons will be, respectively, Fermi-Dirac and Bose-Einstein.

distribution of the neutrinos in the synchronous gauge<sup>2</sup> [4, 5]:

$$\mathcal{F}'_\nu + ik\mu\mathcal{F}_\nu = 2\mu^2(h' + 6\xi') - 4\xi', \quad \mu = \hat{k} \cdot \hat{n}. \quad (2)$$

where, as in the conventional  $\Lambda$ CDM models the neutrinos are massless and, consequently,  $v^i = q^i/|\vec{q}| = n^i$ . The evolution equations of the brightness perturbations of the intensity (i.e.  $\Delta_I$ ) and of the polarization (i.e.  $\Delta_Q$  and  $\Delta_U$ ), can be derived from Eq. (1) (always in the limit  $e \rightarrow 0$ ) by identifying  $\mathcal{C}_{\text{coll}}$  with the electron-photon collision term when the energy of the photons is parametrically smaller than the electron mass and when the electron recoil is neglected:

$$\Delta'_I + (ik\mu + \epsilon')\Delta_I = -\left[\xi' - \frac{\mu^2}{2}(h' + 6\xi')\right] + \epsilon'\left[\Delta_{I0} + \mu v_b - \frac{3\mu^2 - 1}{4}(\mu)\mathcal{S}\right], \quad (3)$$

$$\Delta'_Q + (ik\mu + \epsilon')\Delta_Q = \frac{3\epsilon'}{4}(1 - \mu^2)\mathcal{S}, \quad \Delta'_U + (ik\mu + \epsilon')\Delta_U = 0, \quad (4)$$

where  $\epsilon' = ax_e \tilde{n}_e \sigma_{\text{Th}}$  is the differential optical depth defined in terms of the ionization fraction  $x_e$ , of the electron density, and of the Thompson cross section  $\sigma_{\text{Th}}$ ;  $v_b = \theta_b/(ik)$  is the baryon velocity to be defined in a moment. The source term in Eqs. (3) and (4), i.e.  $\mathcal{S} = (\Delta_{I2} + \Delta_{Q2} + \Delta_{Q0})$ , contains the quadrupole of the intensity of the radiation field,  $\Delta_{I2}$ . In a nutshell, the CMB is linearly polarized (i.e.  $\Delta_Q \neq 0$ ) since the amount of linear polarization is proportional, to first-order in the tight-coupling expansion, to the quadrupole of the intensity which is, in turn, proportional to the first-order dipole. This reasoning can be generalized to include the effects of the magnetohydrodynamical Lorentz force. The one-body distributions for electrons and ions enter Maxwell's equations as

$$\vec{\nabla} \cdot \vec{E} = 4\pi e \int d^3v [f_+(\vec{x}, \vec{v}, \tau) - f_-(\vec{x}, \vec{v}, \tau)], \quad \vec{\nabla} \cdot \vec{B} = 0, \quad (5)$$

$$\vec{\nabla} \times \vec{E} + \vec{B}' = 0, \quad \vec{\nabla} \times \vec{B} - \vec{E}' = 4\pi e \int d^3v \vec{v} [f_+(\vec{x}, \vec{v}, \tau) - f_-(\vec{x}, \vec{v}, \tau)]. \quad (6)$$

For length scales much larger than the Debye scale<sup>3</sup>, and for comoving frequencies smaller than the plasma frequency (i.e.  $\omega \ll \omega_{\text{pe}}$ ), Eqs. (2), (5) and (6) reduce to an effective one-fluid description where the relevant dynamical variables are given by the centre of mass velocity of the electron-ion system (i.e.  $\vec{v}_b = (m_e \vec{v}_e + m_i \vec{v}_i)/(m_e + m_i)$ ) and by the total current  $\vec{J}$ . Ions (i.e. protons) are much heavier than electrons: the obtained equations can be expanded in powers of  $m_e/m_p \ll 1$ . These approximations lead to (resistive) magnetohydrodynamics (MHD) where the electromagnetic disturbances cannot propagate: the total current is solenoidal (i.e., according to Eq. (6),  $4\pi\vec{J} = \vec{\nabla} \times \vec{B}$ ) and the electric fields vanish in the baryon rest frame with an accuracy determined by the inverse of the Coulomb

<sup>2</sup>Recall, for this purpose, that the scalar fluctuation of the geometry  $h_{ij}(\vec{x}, \tau)$  carries two degrees of freedom, i.e., in Fourier space,  $h_{ij}(\vec{k}, \tau) = [\hat{k}_i \hat{k}_j h(k, \tau) + 2\xi(k, \tau)(3\hat{k}_i \hat{k}_j - \delta_{ij})]$ .

<sup>3</sup>The Debye length is defined as  $\lambda_D = \sqrt{T/(8\pi e^2 n_0)}$  with  $n_0 = a^3 \tilde{n}_e \equiv a^3 \tilde{n}_i$  where  $\tilde{n}_e$  and  $\tilde{n}_i$  are the electrons and the ions concentrations.

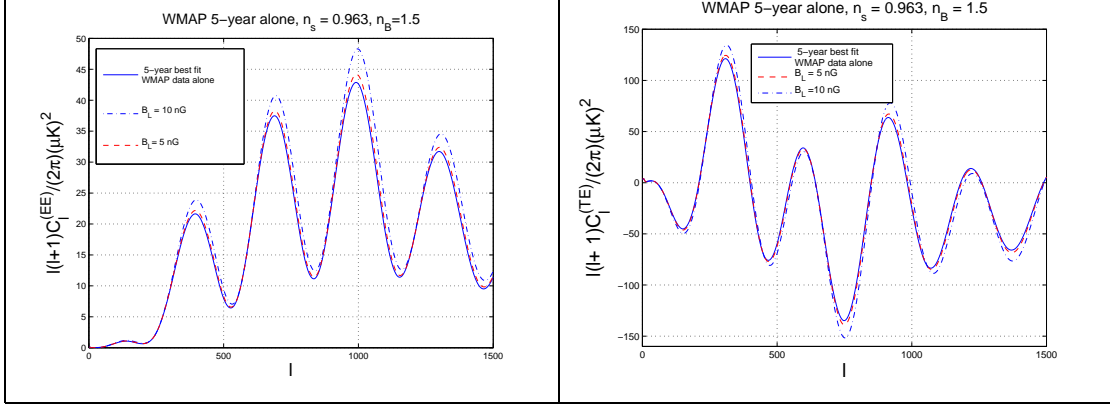


Figure 1: The TE and EE angular power spectra.

conductivity. The Lorentz force affects anyway the dynamics of the photon-baryon fluid:

$$\theta'_{\gamma b} + \frac{\mathcal{H}R_b}{R_b + 1}\theta_{\gamma b} = \frac{3}{4a^4\rho_\gamma}\vec{\nabla} \cdot [\vec{J} \times \vec{B}] - \frac{\nabla^2\delta_\gamma}{4(R_b + 1)}, \quad (7)$$

$$\delta'_\gamma = \frac{2}{3}h' - \frac{4}{3}\theta_{\gamma b}, \quad \delta'_b = \frac{h'}{2} - \theta_{\gamma b}, \quad R_b = \frac{3\rho_b}{4\rho_\gamma}, \quad (8)$$

where, by definition,  $\theta_X = \vec{\nabla} \cdot \vec{v}_X$  is the three divergence of the velocity field and  $\theta_{\gamma b} = \theta_\gamma = \theta_b$ . In Eq. (8)  $\delta_\gamma$  and  $\delta_b$  are the density contrasts of photons and baryons. Both the metric fluctuations and the density contrasts of the various species will enter the corresponding Einstein equations whose explicit form can be found in [4, 5].

The comoving (angular) frequency corresponding to the maximum of the CMB spectrum is  $\bar{\omega}_{\max} = 2\pi\nu_{\max}$  where  $\nu_{\max} = 222.617$  GHz. The comoving plasma frequency is instead  $\bar{\omega}_{\text{pe}} = 0.285$  MHz for  $h_0^2\Omega_{b0} = 0.02273$  (as implied by the best fit to the WMAP 5-year data alone). For CMB photon frequencies  $\bar{\omega} > \bar{\omega}_{\text{pe}}$ , Eq. (1) cannot be reduced to a one-fluid description. The stochastic magnetic field (obeying the one-fluid MHD equations) can then be treated as a background field. The propagation of the electromagnetic disturbances is calculated by taking into account the dynamics of ions and electrons within the cold plasma<sup>4</sup> approximation which is rather safe since  $T_i \ll m_i$  and  $T_e \ll m_e$  and  $g_{\text{plasma}} \ll 1$ . The initial conditions of the Einstein-Boltzmann hierarchy are given in terms of the so-called magnetized adiabatic mode [4, 5] which is a solution of the system formed by Eqs. (7)–(8) (as well as by the other MHD and Einstein equations) in the tight-Thompson coupling approximation. The two sources of inhomogeneity of the system are represented by the stochastic magnetic field (which follows the effective set of one-fluid equations) and by the curvature perturbations.

<sup>4</sup>The plasma parameter [8] is  $g_{\text{plasma}} = (V_D n_0)^{-1}$ , i.e. the inverse of the number of charge carriers inside the Debye sphere. Around decoupling  $g_{\text{plasma}} \simeq 2.3 \times 10^{-7} \sqrt{x_e}$  for the typical value of the baryonic density implied by WMAP 5-year data.

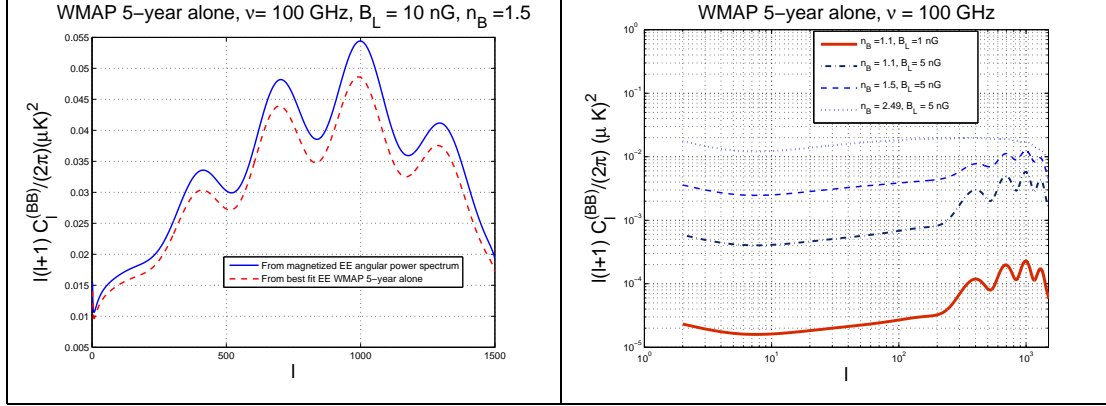


Figure 2: The BB angular power spectra induced by the dispersive propagation of the electromagnetic signal in a magnetized background.

The Fourier amplitudes of the large-scale magnetic field will satisfy:

$$\langle B_i(\vec{k}) B_j(\vec{p}) \rangle = \frac{2\pi^2}{k^3} \mathcal{P}_B(k) P_{ij}(k) \delta^{(3)}(\vec{k} + \vec{p}), \quad \mathcal{P}_B = A_B \left( \frac{k}{k_L} \right)^{n_B-1}. \quad (9)$$

where  $A_B$  is the spectral amplitude,  $n_B$  is the spectral index and  $k_L$  is the magnetic pivot scale;  $P_{ij} = (\delta_{ij} - \hat{k}_i \hat{k}_j)$  the transverse projector. The curvature perturbations will be assigned consistently with the notations of Eq. (9) and, in particular, their power spectrum will be given by  $\mathcal{P}_{\mathcal{R}}(k) = \mathcal{A}_{\mathcal{R}}(k/k_p)^{n_s-1}$  where  $\mathcal{A}_{\mathcal{R}}$  is the spectral amplitude at the pivot scale  $k_p = 0.002 \text{ Mpc}^{-1}$ ;  $n_s$  is the spectral index<sup>5</sup>. Our numerical code extends the code described in [5] and it is based on CMBFAST [7]. As decoupling approaches  $\theta_\gamma \neq \theta_b$  and the linear polarization is generated. For frequencies of the CMB photons much larger than  $\bar{\omega}_{pe}$ , dispersive effect come into play (i.e.  $\theta_e \neq \theta_i$ ) and the linear polarization is rotated<sup>6</sup> leading, ultimately, to the BB angular power spectrum. Such a rotation is proportional to  $\hat{n} \cdot \vec{B}$  where  $\hat{n}$ , as before, is the direction of the photon momentum. The Larmor radius of the electrons and of the ions is much larger than the inhomogeneity scale of the magnetic field: the dynamics of electrons and ions (as well as the dispersion relations [9]) can be studied under the guiding centre approximation pioneered by Alfvén [10]. The two helicities composing the (linear) CMB polarization propagate with different phase (as well as group) velocities. The Faraday rotation rate depends upon the difference  $\bar{\omega}[n_+(\bar{\omega}) - n_-(\bar{\omega})]/2$  where  $n_\pm(\bar{\omega})$  are the refractive indices of the two circularly polarized waves (one with positive helicity and the other with negative helicity). The heat transfer equations are then supplemented, in this

<sup>5</sup>For the  $\Lambda$ CDM paradigm the 5-year WMAP data (alone) imply  $n_s = 0.963^{+0.014}_{-0.015}$ .

<sup>6</sup>There is a second class of dispersive effects which is related to the so-called ordinary and extraordinary waves [8]. The latter dispersion relations are insignificant since the scales of the problem imply that the refractive indices are 1 both for the ordinary and extraordinary waves [9].

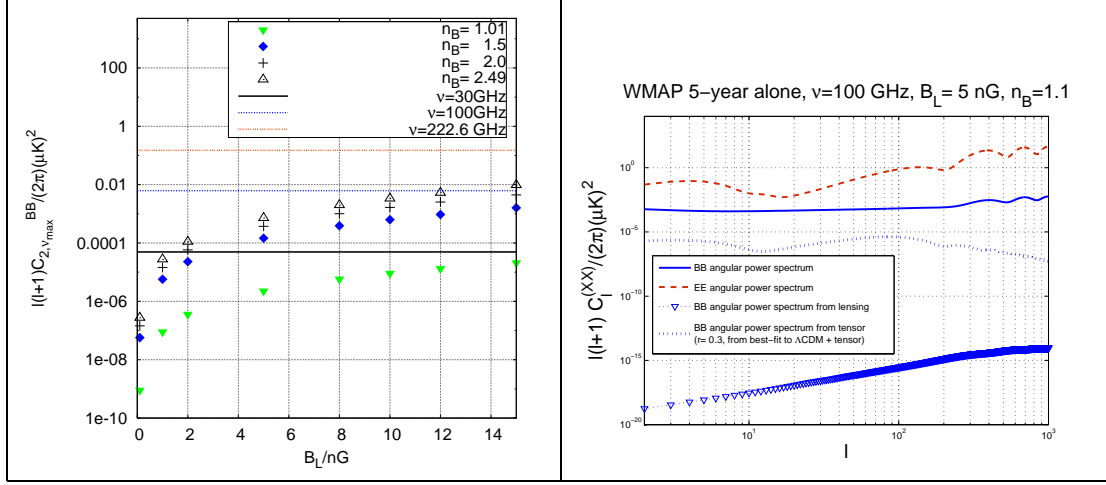


Figure 3: The bound on the BB angular power spectrum from the WMAP 5-year data (plot at the left). At the right, the magnetized EE and BB power spectra are compared to the B-modes expected from lensing and from the tensor mores in the case  $r = 0.3$ .

regime, by the Faraday rotation rate:

$$\Delta'_Q + n^i \partial_i \Delta_Q = 2\epsilon' F(\hat{n}) \Delta_U, \quad \Delta'_U + n^i \partial_i \Delta_U = -2\epsilon' F(\hat{n}) \Delta_Q, \quad (10)$$

where  $F(\hat{n}) = 3/(16\pi^2 e) \hat{n} \cdot \vec{B}/\nu^2$  and  $\nu$  denotes here the comoving frequency. Since the Faraday rate depends upon a stochastic field<sup>7</sup> it will also be characterized by a power spectrum whose explicit form depends upon the spectral amplitude and slope of the magnetic field [12, 9]. In Fig. 1 the EE and TE angular power spectra are reported in the case of the WMAP 5-year data. The TE and EE angular are defined from the corresponding expansion coefficients by recalling that, in the present notations,  $\mathcal{M}_\pm(\hat{n}) = \Delta_Q(\hat{n}) \pm i\Delta_U(\hat{n}) = \sum_{\ell m} a_{\pm 2, \ell m} \pm 2 Y_{\ell m}(\hat{n})$  where  $\pm 2 Y_{\ell m}(\hat{n})$  are the spin-2 spherical harmonics. In terms of  $a_{\pm 2, \ell m}$  the E-mode and the B-mode are given by  $a_{\ell m}^{(E)} = -(a_{2, \ell m} + a_{-2, \ell m})/2$  and by  $a_{\ell m}^{(B)} = i(a_{2, \ell m} - a_{-2, \ell m})/2$ . In Fig. 1 the spectral index as well as all the other parameters of the underlying  $\Lambda$ CDM model have been fixed to the best-fit value of the WMAP-5year data alone. In both plots of Fig. 1 the best fit is illustrated with the full lines. The angular power spectrum of Faraday rotation is defined as  $C_\ell^{(F)} \delta_{\ell\ell' mm'} = \langle a_{\ell m}^* a_{\ell' m'} \rangle$  where  $a_{\ell m} = \int d\Omega_{\hat{n}} Y_{\ell m}(\hat{n})^* F(\hat{n})$ . In terms of  $C_\ell^{(F)}$  the autocorrelation of the B-mode will be given by

$$C_\ell^{(BB)} = \sum_{\ell_1, \ell_2} \mathcal{G}(\ell_1, \ell_2, \ell) C_{\ell_1}^{(F)} C_{\ell_2}^{(EE)}, \quad (11)$$

<sup>7</sup>It is here assumed that spatial isotropy is unbroken (as observations seem to indicate). A *uniform* magnetic field (such as the one assumed in [11]) would break spatial isotropy. If the magnetic field breaks spatial isotropy the TB (and possibly EB) power spectra will be present. In the present case the latter power spectra vanish.

where  $\mathcal{G}(\ell_1, \ell_2, \ell)$  is a function of the multipoles containing a Clebsh-Gordon coefficient [12, 9],  $C_\ell^{(\text{EE})}$  is the angular power spectrum of the polarization autocorrelations and<sup>8</sup>

$$C_\ell^{(\text{F})} = 30.03 \bar{\Omega}_{\text{BL}} \left( \frac{\nu}{\nu_{\text{max}}} \right)^{-4} \left( \frac{k_0}{k_{\text{L}}} \right)^{n_{\text{B}}-1} \frac{\ell(\ell+1)(2\pi)^{n_{\text{B}}-1} \Gamma\left(\frac{5-n_{\text{B}}}{2}\right) \Gamma\left(\ell + \frac{n_{\text{B}}}{2} - \frac{3}{2}\right)}{\Gamma\left(\frac{n_{\text{B}}-1}{2}\right) \Gamma\left(\frac{6-n_{\text{B}}}{2}\right) \Gamma\left(\frac{7}{2} + \ell - \frac{n_{\text{B}}}{2}\right)}, \quad (12)$$

where  $\bar{\Omega}_{\text{BL}} = B_{\text{L}}^2/(8\pi\bar{\rho}_\gamma)$ . In Fig. 2 the BB angular power spectra are reported. In the plot at the left the dashed line shows the result obtainable from Eq. (11) in the case the  $C_\ell^{(\text{EE})}$  would be the one arising in the context of the  $\Lambda$ CDM adiabatic mode. The WMAP 5-year data (see, in particular, [2]) imply that, when averaged over  $\ell = 2 - 6$ ,  $\ell(\ell+1)C_\ell^{(\text{BB})}/(2\pi) < 0.15(\mu\text{K})^2$  (95 % C.L.). The putative constraint of [2] does not make reference to a specific frequency. So it should be imposed at the lowest frequency channel. The lowest available frequency for this purpose would be for 27 GHz. The preceding frequency (i.e. 23 GHz) has been used as a foreground template and, consequently, the EE and BB power spectra have not been freed from the foreground contamination. We therefore choose to set the bound for a minimal frequency of 30 GHz since this is not only intermediate between the KKa and KQ bands of the WMAP experiment but it is also the putative (lowest) frequency of the Planck experiment [13]. In Fig. 3 (plot at the left) the full, dashed and dot dashed lines refer, respectively, to the cases of  $\nu = 30$  GHz,  $\nu = 100$  GHz and  $\nu = \nu_{\text{max}}$ . In the right plot of Fig. 3 the magnetized EE and BB power spectra are compared with the B-modes from the lensing of CMB anisotropies and from the B-modes induced by the tensor modes (in the case of tensor-to-scalar ratio 0.3 which is the best fit value of the  $\Lambda$ CDM model plus tensors to the WMAP 5-year data). As it is apparent from Fig. 3 the constraints on the B-mode are not stringent for the magnetized background and are safely satisfied by a nG field at the epoch of the gravitational collapse<sup>9</sup>. The constraints on the height of the acoustic peaks are comparatively more stringent [5, 9].

The obtained results suggest that multifrequency measurements of the CMB temperature and polarization within different channels will permit, for instance with Planck [13], an accurate scrutiny of the possible presence of magnetized birefringence. For this purpose, the scaling properties of the temperature and polarization autocorrelations in different frequency channels should be analyzed and compared. While  $C_\ell^{(\text{BB})}$  should scale as  $\nu^{-4}$ , the EE and TT power spectra will be frequency independent [9].

K.E.K. is supported by the “Ramón y Cajal” program and by the grants FPA2005-04823, FIS2006-05319 and CSD2007-00042 of the Spanish Science Ministry.

---

<sup>8</sup>For illustrative purposes we will limit our attention on the case  $n_{\text{B}} > 1$ ; in this situation  $A_{\text{B}} = (2\pi)^{n_{\text{B}}-1} \Gamma((n_{\text{B}}-1)/2) B_{\text{L}}^2$ .

<sup>9</sup>The WMAP collaboration reports also limits on axion-induced birefringence. As discussed in [9] these bounds are obtained by assuming that the birefringence is independent on the frequency of the incoming polarization (which is not true in the case of the magnetic field). Furthermore, the rate of axion-induced birefringence is fully homogeneous which is opposite to the case considered here.

## References

- [1] M. Giovannini, Int. J. Mod. Phys. D **13**, 391 (2004) ; A. Brandenburg and K. Subramanian, Phys. Rept. **417**, 1 (2005); J. D. Barrow, R. Maartens and C. G. Tsagas, Phys. Rept. **449**, 131 (2007).
- [2] M. R. Nolte *et al.* [WMAP Collaboration], arXiv:0803.0593 [astro-ph]; E. Komatsu *et al.* [WMAP Collaboration], arXiv:0803.0547 [astro-ph].
- [3] K. Subramanian and J. D. Barrow, Phys. Rev. Lett. **81**, 3575 (1998); Mon. Not. Roy. Astron. Soc. **335**, L57 (2002); K. Subramanian, T. R. Seshadri and J. D. Barrow, Mon. Not. Roy. Astron. Soc. **344**, L31 (2003).
- [4] M. Giovannini, Phys. Rev. D **73**, 101302 (2006); Phys. Rev. D **74**, 063002 (2006); PMC Phys. A **1**, 5 (2007); Class. Quant. Grav. **23**, 4991 (2006).
- [5] M. Giovannini and K. E. Kunze, Phys. Rev. D **77**, 061301 (2008); Phys. Rev. D **77**, 063003 (2008); arXiv:0802.1053 [astro-ph].
- [6] E. Bertschinger, arXiv:astro-ph/9506070; C. P. Ma and E. Bertschinger, Astrophys. J. **455**, 7 (1995).
- [7] U. Seljak and M. Zaldarriaga, Astrophys. J. **469**, 437 (1996); M. Zaldarriaga, D. N. Spergel and U. Seljak, Astrophys. J. **488**, 1 (1997).
- [8] N. Krall, A. Trivelpiece, *Principles of Plasma Physics*, (San Francisco Press, 1986).
- [9] M. Giovannini and K. E. Kunze, in preparation.
- [10] H. Alfvén, *Cosmical Electrodynamics* (Clarendon press, Oxford, 1951).
- [11] A. Kosowsky and A. Loeb, Astrophys. J. **469**, 1 (1996); M. Giovannini, Phys. Rev. D **56**, 3198 (1997); C. Scoccola, D. Harari and S. Mollerach, Phys. Rev. D **70**, 063003 (2004).
- [12] L. Campanelli, A. D. Dolgov, M. Giannotti and F. L. Villante, Astrophys. J. **616**, 1 (2004); A. Kosowsky, T. Kahniashvili, G. Lavrelashvili and B. Ratra, Phys. Rev. D **71**, 043006 (2005).
- [13] <http://www.rssd.esa.int/index.php?project=PLANCK> .